PE_PGRS3 of *Mycobacterium tuberculosis* is specifically expressed at low phosphate concentration and its arginine-rich C-terminal domain mediates adhesion and persistence in host tissues when expressed in *Mycobacterium smegmatis*.

Flavio De Maio[1¶], Basem Battah[1,2¶], Valentina Palmieri[3], Linda Petrone[4], Francesco Corrente[5], Alessandro Salustri[1], Ivana Palucci[1], Silvia Bellesi[5], Massimiliano Papi[3], Salvatore Rubino[2], Michela Sali[1], Delia Goletti[4], Maurizio Sanguinetti[1], Riccardo Manganelli[6], Marco De Spirito[3], and Giovanni Delogu[1]*

[1]Institute of Microbiology, Università Cattolica del Sacro Cuore – IRCCS Fondazione Policlinico Universitario Gemelli, Rome;

[2]Department of Biomedical Sciences, University of Sassari;

[3]Institute of Physics, Università Cattolica del Sacro Cuore – IRCCS Fondazione Policlinico Universitario Gemelli, Rome;

[4]Translational Research Unit, Department of Epidemiology and Preclinical Research, National Institute for Infectious Diseases, L. Spallanzani, Rome;

[5]Institute of Haematology, Università Cattolica del Sacro Cuore – IRCCS Fondazione Policlinico Universitario Gemelli, Rome;

[6]Department of Molecular Medicine, University of Padua, Padua

[¶] These authors have contributed equally to this work

This article has been accepted for publication and undergone full peer review but has not been through the copyediting, typesetting, pagination and proofreading process which may lead to differences between this version and the Version of Record. Please cite this article as doi: 10.1111/cmi.12952

* Corresponding author: Giovanni Delogu, PhD. Institute of Microbiology, Università Cattolica del Sacro Cuore – Fondazione Policlinico Universitario Gemelli, Largo A. Gemelli, 8 – 00168 - Rome, Italy. Tel. ++390630154964; Email: giovanni.delogu@unicatt.it

Keywords: Mycobacterium tuberculosis, PE_PGRS, phosphate, adhesion.

Abstract

PE_PGRSs of *Mycobacterium tuberculosis* (*Mtb*) represent a family of complex and peculiar proteins whose role and function remain elusive. In this study, we investigated PE_PGRS3 and PE_PGRS4, two highly homologous PE_PGRSs encoded by two contiguous genes in the *Mtb* genome. Using a gene-reporter system in *Mycobacterium smegmatis* (*Ms*) and transcriptional analysis in *Mtb*, we show that PE_PGRS3, but not PE_PGRS4, is specifically expressed under low phosphate concentrations. Interestingly, PE_PGRS3, but not PE_PGRS4, has a unique, arginine-rich C-terminal domain of unknown function. Heterologous expression of PE_PGRS3 in *Ms* was used to demonstrate cellular localization of the protein on the mycobacterial surface, where it significantly affects net surface charge. Moreover, expression of full-length PE_PGRS3 enhanced adhesion of *Ms* to murine macrophages and human epithelial cells and improved bacterial persistence in spleen tissue following infection in mice. Expression of the PE_PGRS3 functional deletion mutant lacking the C-terminal domain in *Ms* did not enhance adhesion to host cells, showing a phenotype similar to the *Ms* parental strain. Interestingly, enhanced persistence of *Ms* expressing PE_PGRS3 did not correlate with increased concentrations of inflammatory cytokines. These results point to a critical role for the ≈ 80 amino acids long, arginine-rich C-terminal domain of PE_PGRS3 in tuberculosis pathogenesis.

Introduction

Tuberculosis (TB) remains one of the most important infectious diseases in the world with 1.7 million deaths and 10.4 million new cases estimated in 2016 (World Health Organization, 2017). The co-infection with the human immunodeficiency virus (HIV), the spread of multidrug-resistant (MDR-TB) and extensively drug resistant (XDR-TB) *Mycobacterium tuberculosis* (*Mtb*) strains are a cause of major concern for public health authorities (World Health Organization, 2017). For these reasons, there is a need for a better vaccine, new drugs and improved diagnostics.

It is widely accepted that to design and develop new tools to fight TB, a better understanding of the *Mtb* biology and mechanism of pathogenesis is needed (Bottai *et al.*, 2014; Delogu *et al.*, 2014; Pai *et al.*, 2016). The genes that make *Mtb* capable to persist in the host after primary infection and the mechanisms responsible for the infection reactivation remain poorly understood, although it is clear that *Mtb* presents a remarkable adaptation against various physiological and environmental stresses, including those induced by drugs (Barry, III *et al.*, 2009; Boutte and Crosson, 2013; Cardona, 2009; Fattorini *et al.*, 2013; Gengenbacher and Kaufmann, 2012; Peddireddy *et al.*, 2017; Weiss and Schaible, 2015).

A peculiar feature of *Mtb* is certainly the presence of two large protein families (PE and PPE), which are restricted to few mycobacteria causing disease in humans and mammals (Brennan and Delogu, 2002; Cole *et al.*, 1998). The genes coding for these proteins account for almost 8% of the genome coding capacity and were shown to be responsible for most of the genetic variability of *Mtb* (Cole *et al.*, 1998). *pe_pgrs* genes emerged in the slow-growing mycobacteria only after the advent of the ESX-5 type 7 secretion system (T7SS) (Gey van Pittius *et al.*, 2006) and co-evolved since then with ESX-5 through a process of multiple gene duplication and diversification events in MTBC, *M. marinum* and *M. ulcerans* (Delogu *et al.*,

2017). Several studies showed that surface localization of PE/PPE proteins, including PE_PGRSs, is ESX-5 dependent, providing a functional support to the evolutionary scenario (Gey van Pittius *et al.*, 2006; Abdallah *et al.*, 2007; Abdallah *et al.*, 2009; Houben *et al.*, 2012). The role of ESX-5 in PE_PGRS secretion and surface localization has been questioned in *Mtb* (Bottai *et al.*, 2012), albeit very recent data indicate that *Mtb* strains mutants for the *ppe38* gene are unable to secrete PE_PGRSs and show enhanced virulence in mice (Ates *et al.*, 2018). Interestingly, hypervirulent *Mtb* strains belonging to the Beijing clade present a mutated *ppe38* gene and are unable to secrete PE_PGRSs (Ates *et al.*, 2018). While more experiments are needed to dissect the relationship between ESX-5 and PE_PGRSs secretion/surface localization and the role of the latter in *Mtb* virulence, the biological mechanisms whereby PE_PGRSs exert their role remains poorly characterized.

The functional studies on PE_PGRSs have been hampered by the lack of tools and by the redundancy of these genes in *Mtb*. The expression of the recombinant protein in *Mycobacterium smegmatis*, which does not possess any *pe_pgrs* or an ESX-5 secretion system, has been widely used to investigate these proteins and the results obtained have provided some relevant information. For example, PE_PGRS60 and PE_PGRS61 were shown to bind extracellular components (Monu and Meena, 2016); PE_PGRS33 was shown to interact with TLR2 to mediate inflammatory responses and entry in macrophages (Palucci *et al.*, 2016; Zumbo *et al.*, 2013); PE_PGRS18 and PE_PGRS41 were shown to increase mycobacteria survival within macrophages by interfering with innate host immune responses (Deng *et al.*, 2017; Yang *et al.*, 2016); PE_PGRS47 inhibited autophagy and interfered with the MHC class-II antigen presentation pathway (Saini *et al.*, 2016); PE_PGRS17, PE_PGRS30, PE_PGRS33 and PE_PGRS62 were shown to modulate cytokines secretion (Chatrath *et al.*, 2016; Chen *et al.*, 2013; Ying Huang, 2010; Zumbo *et al.*, 2013).

In this current study, we present the characterization of two PE_PGRSs which have been selected because of their similarity and their localization in the genome region coding for the ESX3 secretion system (Serafini *et al.*, 2009; Serafini *et al.*, 2013; Tufariello *et al.*, 2016). PE_PGRS3 (Rv0278c) and PE_PGRS4 (Rv0279c) share a similar PE_PGRSs amino acid sequence, characterized by the presence of two GRPLI motifs, one immediately upstream of the PGRS domain and the second in the PGRS domain. However, PE_PGRS3 is characterized by a unique arginine rich C-terminal domain. These two genes were expressed and characterized in *Mycobacterium smegmatis* (*Ms*) to investigate the pattern of gene expression and their biological function.

Results

Inorganic phosphate starvation induces PE_PGRS3, but not PE_PGRS4, expression. To start investigating the role of PE_PGRS3 and PE_PGRS4 in the biology of *Mtb*, the two corresponding genes (Figure 1, S1), including their respective putative promoters, were amplified from the *Mtb* H37Rv genome, cloned in two pMV-based vectors upstream of the sequences coding either the Green Fluorescent Protein (GFP) or the haemagglutinin (HA) epitope (Table S2). The *Ms* recombinant strain expressing the GFP-tagged PE_PGRS4 (MsPE_PGRS4^{GFP}) showed intense fluorescence when grown in complete 7H9 medium, while the *Ms*PE_PGRS3^{GFP} did not (data not shown). To assess whether PE_PGRS3 expression, or stability of the corresponding protein, required a concomitant expression of PE_PGRS4, the two neighbouring genes were co-expressed by electroporating *Ms* with the two plasmids to generate *Ms*PE_PGRS3^{GFP}/PE_PGRS4^{HA} and *Ms*PE_PGRS4^{GFP}/PE_PGRS3^{HA} (Table S2). The recombinant *Ms* strains were grown as previously described and then analysed by fluorescence microscopy. *Ms*PE_PGRS4^{GFP}/PE_PGRS3^{HA} showed an intense fluorescence while the *Ms*PE_PGRS3^{GFP}/PE_PGRS4^{HA} did not (data not shown). Immunoblot analysis with

anti-GFP and anti-HA specific antibodies carried out on whole cell lysates obtained from *Ms*PE_PGRS3^{GFP}, *Ms*PE_PGRS4^{GFP}, *Ms*PE_PGRS3^{GFP}/PE_PGRS4^{HA} and *Ms*PE_PGRS4^{GFP}/PE_PGRS3^{HA} demonstrated the presence of bands corresponding to PE_PGRS4 (~ 95 KDa and ~ 79 KDa when tagged with GFP and HA, respectively), while no signal corresponding to the PE_PGRS3-based chimaeras were detected (Figure S2).

To assess whether expression of PE_PGRS3 requires specific environmental conditions, the *Ms* recombinant strains were grown in conditions known to mimic stimuli encountered by *Mtb* during infection (Betts *et al.*, 2002; Elks *et al.*, 2013; Gengenbacher *et al.*, 2010; Lim *et al.*, 1999; Wayne, 1954; Wayne, 2001). The *Ms* recombinant strains were cultured in Sauton medium under low oxygen concentration, acidic pH, phosphate, iron or magnesium starvation, and at different time points bacteria were analysed by fluorescence microscopy to detect GFP expression. Interestingly, while PE_PGRS4^{GFP} was expressed under all conditions tested, the *Ms*PE_PGRS3^{GFP} and *Ms*PE_PGRS3^{GFP}/PE_PGRS4^{HA} showed a significant fluorescence only when cultured in low phosphate (P_i) medium for at least 15 days (Figure S3). These findings suggest that PE_PGRS3 is expressed following long-term growth in low P_i environment. To test this hypothesis, recombinant strains were grown until mid-log phase and then sub-inoculated in low P_i or standard P_i Sauton medium and incubated up to 15 days, when bacteria were plated on chamber slides and fixed before confocal fluorescence analysis. The recombinant *Ms* strains expressing PE_PGRS33^{GFP} and native GFP under the control of the *pe_pgrs33* and *hsp60* promoters (Cascioferro *et al.*, 2011; De Maio *et al.*, 2014; Delogu *et al.*, 2004b), respectively, were included as controls. Expression of PE_PGRS4^{GFP}, PE_PGRS33^{GFP} and cytosolic GFP was observed in both low and standard P_i concentrations, while PE_PGRS3^{GFP} was expressed only when bacteria were cultured in low P_i (Figure 2A). Fluorescence quantification analysis highlighted that emission of *Ms*PE_PGRS3^{GFP} (at low P_i) and *Ms*PE_PGRS4^{GFP} strains were slightly lower than *Ms*PE_PGRS33^{GFP}. Furthermore, non-

significant differences in fluorescence emission were observed between *Ms*PE_PGRS4^{GFP} and *Ms*PE_PGRS33^{GFP} cultured in low or standard P_i (Figure 2B). Taken together, these results demonstrate that PE_PGRS3 and PE_PGR4 are differently expressed, and that an environment poor in P_i triggers PE_PGRS3 expression.

To investigate the kinetic of PE_PGRS3 expression under low P_i condition, the recombinant GFP-tagged strains were analyzed by flow cytometry. Briefly, the mycobacterial strains were grown until mid-log phase in complete 7H9 medium and then sub-inoculated in low P_i Sauton medium. Interestingly, the percentage of fluorescence intensity of mycobacteria expressing PE_PGRS3^{GFP} increased from 0% (day 1) to 2.5% at day 15 of incubation, when the addition of P_i to the medium promptly reduced PE_PGRS3 expression. No significant changes were observed in the other recombinant strains tested (Figure 3). These results indicate that P_i regulates the expression of PE_PGRS3.

Induction of *pe_pgrs3* expression correlates with *relA* in *Ms* and *Mtb*. Mycobacterial adaptation to low P_i includes the stringent response, a complex biological process leading to a profound variation of bacterial metabolism mainly mediated by the alarmone ppGpp, whose intracellular levels are regulated by the GTP pyrophosphokinase RelA (Boutte and Crosson, 2013; Manganelli, 2014; Primm *et al.*, 2000; Rifat *et al.*, 2009;Tischler *et al.*, 2013). To understand whether the *pe_pgrs3* transcriptional profile correlated with that of *relA*, transcriptional analysis by reverse-transcriptase real time PCR was carried out on total RNA extracted from *Ms*PE_PGRS3^{GFP} cultured in standard and low P_i conditions. Transcriptional analysis showed that both genes were indeed upregulated after 15 days of culture in low Pi medium (Figure 4A). The variation of the expression profiles of *pe_pgrs*3 and *relA* following culture in low Pi conditions were also assessed in *Mtb* H37Rv (Figure 4B). Both genes were up-regulated after 30 days of culture. However, no differential expression was observed after

7 and 15 days of culture. Since the alternative sigma factor SigE is involved in the development of the stringent response, we repeated this experiment in an *Mtb* mutant where this gene was deleted (Casonato *et al.*, 2014; Manganelli *et al.*, 2001; Manganelli, 2014). Interestingly, the induction of both *pe_pgrs3* and *relA* in this strain started earlier and was stronger than that observed in the wild type (Figure 4C), confirming a role of SigE in the complex regulatory network leading to stringent response. Taken together these results indicate that *pe_pgrs3* is upregulated after long-term culture at low P_i conditions and its expression profile in *Mtb* is analogous to *relA*.

PE_PGRS3 in *Ms* is surface exposed and affects the cell surface charge. The expression profile observed for *pe_pgrs3* indicates that *Mtb*, or a recombinant *Ms* strain expressing *pe_pgrs3* under the control of its own promoter, would express very low level of PE_PGRS3 in *in vitro* experimental settings involving the use of eukaryotic cells. Hence, to investigate the role of PE_PGRS3 during host-pathogen interactions, we developed a tailored genetic system. The new vector was designed to contain two genes: one expressing either the HA-tagged PE_PGRS3, or the functional deletion mutant lacking the arginine-rich C-terminal domain, under the control of the *hbh*A promoter (Delogu *et al.*, 2004a); the second, expressing GFP under the control of the *Ag85b* promoter (Figure S3). These pMV-based vectors were used to transform *Ms* (Figure 5A).

Proper expression of PE_PGRS3, and of its functional mutant *Ms*^{GFP}PE_PGRS3ΔCT^{HA}, were demonstrated by immunoblots carried out on whole cell lysates of recombinant *Ms* strains cultured in standard Sauton media (Figure 5C). No differences in growth pattern between the three strains (*Ms*^{GFP}, *Ms*^{GFP}PE_PGRS3^{HA} and *Ms*^{GFP}PE_PGRS3ΔCT^{HA}) were observed (Figure 5B).

Overexpression of an otherwise poorly expressed PE_PGRS protein may impact cell morphology (Delogu *et al.*, 2004b). Confocal images of recombinant *Ms* strains expressing PE_PGRS3^{HA} (*Ms*^{GFP}PE_PGRS3^{HA}), PE_PGRS3ΔCT^{HA} (*Ms*^{GFP}PE_PGRS3ΔCT^{HA}) and as a control cytosolic GFP (*Ms*^{GFP}) were analyzed by ImageJ to measure cell size (figure 5A and D). Interestingly, mycobacteria expressing the full-length PE_PGRS3 protein were smaller in size (up to 50%) than the control strain (*Ms*^{GFP}) or *Ms*^{GFP}PE_PGRS3ΔCT^{HA} (Figure 5D), which could suggest an impact of the C-terminal domain on the cell size control when PE_PGRS3 is over-expressed.

Given the unique features of the arginine-rich C-terminal domain of PE_PGRS3, proteinase K protection experiments were performed to assess its localization on the mycobacterial surface. As shown in figure 5B, treatment with proteinase K degraded full-length and mutant protein, suggesting that the arginine-rich C terminal domain and the PGRS domain of PE_PGRS3 are available on the mycobacterial surface, in line with previous findings (Cascioferro *et al.*, 2007; Cascioferro *et al.*, 2011; Delogu *et al.*, 2004b) (Figure 5E).

Over-expression on the mycobacterial surface of a highly positively charged peptide, as is the case of the PE_PGRS3 C-terminal domain, may potentially affect the net bacterial surface charge, which is classically negative (Dickson and Koohmaraie, 1989; Hyyrylainen *et al.*, 2007; Silhavy *et al.*, 2010). Zeta potential measurements performed on the three recombinant *Ms* strains indicated that the *Ms*^{GFP}PE_PGRS3^{HA} strain had a Z potential of ≈ -34.7 ± 1.2 mV, which was significantly lower than that of the control strain *Ms*^{GFP} (≈ -47.1 ± 3.1 mV) and the recombinant strain expressing the *Ms*^{GFP}PE_PGRS3ΔCT^{HA} (≈ -41.7 ± 1.9 mV) (Figure 5F). Taken together these results indicate that the arginine-rich C-terminal domain of PE_PGRS3 is available on the mycobacterial surface where it can influence the bacterial net surface charge.

***Ms* expressing PE_PGRS3 shows enhanced adhesion to macrophages and alveolar epithelial cells.** Positively-charged protein domains exposed on the bacterial surface may serve different functions, including the possibility to mediate the adhesion of bacteria to proteoglycans, components of the extracellular matrix or receptors on eukaryotic cells (Delogu and Brennan, 1999). To investigate the potential role of PE_PGRS3 in host-pathogen interaction, and specifically in mediating bacterial entry in the host cells, murine macrophages (J774) and human alveolar epithelial cells (A549) were infected with the previously described *Ms* recombinant strains (*Ms*^{GFP}PE_PGRS3^{HA}, *Ms*^{GFP}PE_PGRS3ΔCT^{HA} and *Ms*^{GFP}), and bacterial counts determined after 4 hours post-infection. As shown in Figure 6A, bacterial association to eukaryotic cells was 10-fold higher for the *Ms* expressing full-length PE_PGRS3 compared to *Ms* control or *Ms* expressing PE_PGRS3ΔCT^{HA}. Confocal microscopy analysis was used to assess the relative number of infected cells at 4 h post-infection. As shown in figure 6B-C, a higher percentage of infected cells, in macrophages and alveolar epithelial cells, was observed for the *Ms*^{GFP}PE_PGRS3^{HA} compared to the other two strains. A similar infection experiment was repeated by adding the antibiotic gentamicin, after washing at 2 h post-infection, to selectively kill the extracellular bacteria. In this setting, only intracellular bacteria would be measured, while bacteria adhering to the cells would be killed by the antibiotic. As shown in figure 6D, the macrophages infected with *Ms*^{GFP}PE_PGRS3^{HA} contained 10 times more intracellular CFUs compared to those infected with the other two *Ms* strains after 6 or 4 days of infection. Conversely, no differences in intracellular CFUs were observed among the A594 cells infected with either of the three strains. Taken together these results indicate that the C-terminal domain of PE_PGRS3 may play a relevant role in the interaction of mycobacteria with its host by promoting adhesion to macrophages and epithelial cells, though the enhanced adhesion is followed by an enhanced bacterial entry in macrophages but not in A549 cells.

PE_PGRS3 expression enhanced *Ms* spleen colonization in mice. To further assess the impact of PE_PGRS3, and of its arginine-rich C terminal domain, on mycobacterial infection, we relied on a *in vivo* model widely used to investigate *Mtb* proteins and specifically PE_PGRSs (Dheenadhayalan *et al.*, 2006a; Singh *et al.*, 2008; Zumbo *et al.*, 2013). C57Bl/6 mice were intraperitoneally infected with the *Ms*^{GFP}PE_PGRS3^{HA}, *Ms*^{GFP}PE_PGRS3ΔCT^{HA} and *Ms*^{GFP} strains ($2x10^7$ CFUs/ml). After 2 and 6 days of infection mice were sacrificed and spleens harvested to determine the bacterial burden. Interestingly, no differences in the spleen size between the three groups of mice were observed (Figure 7A). As shown in figure 7B, spleen CFUs were higher in mice infected with *Ms*^{GFP}PE_PGRS3^{HA}, compared to mice infected with *Ms*^{GFP}PE_PGRS3ΔCT^{HA} and *Ms*^{GFP}, at both times post infection. The inflammatory status of infected mice was assessed by determining a panel of cytokines (IL-1β, IL-6, IL-10, IL-17a, TNFα and INFγ) in the spleen homogenates. As shown in figure 7C, no significant differences were observed between the three groups of mice. Taken together these results indicate that the *Ms* strain expressing full length PE_PGRS3 had enhanced persistence in the spleen compared to the *Ms* strain expressing the functional deletion mutant lacking the C-terminal domain of PE_PGRS3 and the *Ms* control. However, the enhanced persistence of the *Ms*^{GFP}PE_PGRS3^{HA} does not correlate with enhanced inflammation.

Discussion

PE_PGRSs are surface exposed proteins restricted to MTB complex and few other pathogenic mycobacteria that have been implicated in the interaction with host components (Brennan *et al.*, 2001; Brennan and Delogu, 2002; Cole *et al.*, 1998; Espitia *et al.*, 1999). The amino acid sequence and structural homology among the 51 PE_PGRS proteins expressed by *Mtb* initially

suggested a functional redundancy; however, several experimental studies recently indicated that each PE_PGRS protein may play a specific and peculiar role in *Mtb* pathogenesis (Delogu *et al.*, 2006; Delogu *et al.*, 2017; Dheenadhayalan *et al.*, 2006b). Hence, an understanding on the role of PE_PGRS proteins will come by retrieving information on every single PE_PGRS. In this study, we investigated two *pe_pgrs* genes, Rv0278c and Rv0279c, expressing PE_PGRS3 and PE_PGRS4, respectively. These two genes are localized in the *Mtb* genome immediately up-stream of the gene cassette coding the ESX-3 type seven secretion system (T7SS), which has been involved in iron metabolism and *Mtb* pathogenesis (Serafini *et al.*, 2013; Tufariello *et al.*, 2016). These two adjacent genes are highly homologous and represent an example of gene duplication, with each gene with its own putative promoter sequence (Delogu *et al.*, 2017; Gey van Pittius *et al.*, 2006). A major difference between the two proteins is the presence in PE_PGRS3 of a unique arginine rich C-terminal domain. Interestingly, the genome locus containing *pe_pgrs3* was shown to be a recombination hot spot and subject to genomic rearrangements in *Mtb* lineages 1, 3 and 4 (Phelan *et al.*, 2016). The observation that two copies of the *pe_pgrs3* gene are found in *M. canetti* and *M. bovis* but only one in *Mtb*, may have evolutionary and pathogenic implications which deserve further investigation, with a special focus on the functional role of the arginine-rich C-terminal domain.

A main finding of this study is that expression of *pe_pgrs3*, but not of *pe_pgrs4*, is regulated by P_i concentration. Using an *Ms* model of heterologous expression, we demonstrated that expression of *pe_pgrs3* is very low and undetectable under classical growth conditions, but that long term exposure to low P_i triggers its expression. These results were also confirmed by transcriptional analysis in *Mtb*, suggesting that P_i concentration regulates the expression of *pe_pgrs3 in vivo*. P_i is an essential nutrient involved in key biological processes and it has been shown that during bacterial persistence in the lung *Mtb* encounters an environment poor in P_i (Rifat *et al.*, 2009). Moreover, once bacteria reside inside the phagosomal compartment in

macrophages, P_i is a limiting nutrient, particularly in the foamy macrophages where *Mtb* survives and replicates by utilizing host cholesterol, which lacks phosphorous (Elliott and Tischler, 2016a; Rengarajan *et al.*, 2005; Russell *et al.*, 2009). P_i limitation is known to trigger many metabolic changes in mycobacteria, including activation of the stringent response, induction of the non-replicating-persistent state, modulation of the capsular polysaccharide and secretion systems (Elliott and Tischler, 2016b; Rifat *et al.*, 2009; van de Weerd *et al.*, 2016). Recently, it has been shown that hypersecretion by the ESX-5 T7SS in P_i-limiting conditions is mediated by the Pst/SenX3-RegX3 system, which also induces hypersecretion by ESX-1 while lowering secretion of other proteins such as Ag85 (Elliott and Tischler, 2016b). The authors suggested that P_i-limitation in phagosomes may be a signal for *Mtb* to activate the T7SSs known to be involved in virulence to manipulate phagosome function (Elliott and Tischler, 2016b). The finding that *pe_pgrs3* is induced in P_i limiting conditions with a temporal profile that correlates with that of *relA*, indicates that PE_PGRS3 may be included in the pool of secreted and surface antigens expressed during the activation of the stringent response or in response to the sensing of the harsh environment encountered by *Mtb* inside the phagosome. Nevertheless, a finer characterization of the *pe_pgrs3* expression profile in relevant *in vivo* and *in vitro* models that mimic the P_i limiting conditions encountered by *Mtb* in host tissues is needed.

It has been previously shown that PE_PGRS3 is expressed at higher levels in the *Mtb pho*P mutant compared to wild type *Mtb*, with bacterial cells of the former found smaller in size compared to those of the latter (Walters *et al.*, 2006). These findings are consistent with our observation that over-expression of PE_PGRS3 in *Ms* results in bacterial cells of smaller size. Interestingly, over-expression of the PE_PGRS3ΔCt did not affect the bacterial cell size, indicating a critical role played by the 77 amino acids long-, arginine-rich-, surface exposed-C-terminal domain of the protein. P_i starvation in some bacteria has been shown to lead to cell

elongation and changes in cell shape that may serve to increase surface area and maximize P_i uptake (Lamarche *et al.*, 2008). The smaller cells observed in *Ms* over-expressing PE_PGRS3 may suggest a role of this protein in P_i uptake by mycobacteria, although studies in *Mtb*, where uptake of phosphate occurs at 10 to 40 times slower pace compared to *Ms* (Song and Niederweis, 2012), are needed to support this hypothesis.

Indeed, the recombinant *Ms* strain expressing PE_PGRS3, but not PE_PGRS3ΔCT, showed superior ability to adhere to macrophages and human alveolar epithelial cells compared to wild type *Ms,* suggesting that the availability of the arginine-rich C-terminal domain on the mycobacterial surface increases the tropism to host cells. This is different to what was previously observed for HBHA, a mycobacterial surface antigen with a positively charged C-terminus lysine-rich domain that promotes the bacterial adhesion and entry specifically to non-phagocytic cells (Biet *et al.*, 2007;Menozzi *et al.*, 1998;Pethe *et al.*, 2001). Whether the arginine-rich domain of PE_PGRS3 interacts with specific protein receptors or with lipids on host cell surface remains to be determined.

Future studies with *Mtb* are needed to address this issue, though the expression profile observed for PE_PGRS3 will make difficult to investigate the role of this protein in the commonly used experimental conditions.

In previous studies, enhanced persistence in host tissues of *Ms* strains expressing PE_PGRSs correlated with an increased inflammatory response as measured by the enlargement of the spleen and higher levels of cytokines as TNF-α (Dheenadhayalan *et al.*, 2006a; Espitia *et al.*, 1999; Singh *et al.*, 2008), supporting the immunomodulatory role of PE_PGRSs in TB pathogenesis (Camassa *et al.*, 2017; Palucci *et al.*, 2016). Here, the enhanced persistence in the spleen tissue of the *Ms* recombinant strain expressing PE_PGRS3 compared to the parental strain and the *Ms* expressing PE_PGRS3ΔCT, did not correlate with an increase in the inflammatory parameters as indicated by the cytokines secreted and lack of spleen enlargement.

Other PE_PGRSs proteins have been shown to promote increased persistence in host tissues when expressed in *Ms* while attenuating, rather than inducing, inflammation (Deng *et al.*, 2017; Yang *et al.*, 2016), highlighting the fact that different PE_PGRSs may induce different mechanisms to manipulate host responses and enhance bacterial persistence. Our results indicate a key role for the ≈ 80 amino acids long, arginine-rich, C-terminal domain of PE_PGRS3 in TB pathogenesis.

There are some issues that remain to be understood, including the question on how PE_PGRSs can reach the mycobacterial surface despite the lack of ESX-5, which in *Mtb* and *M. marinum* has been implicated in PE_PGRSs secretion and cellular localization (Abdallah *et al.*, 2009; Bottai *et al.*, 2012). The fact that surface localization of several PE_PGRSs in *Ms* has been demonstrated by different research groups, indicates that PE_PGRSs can translocate to the mycobacterial surface in mycobacteria lacking ESX-5, although efficiency of translocation and protein stability is somehow impaired compared to what observed in *Mtb* or BCG (Cascioferro *et al.*, 2011b). We cannot rule out that other ESX systems may compensate in *Ms* the lack of ESX-5 to mediate PE_PGRSs translocation. The characterization of the molecular events and protein components involved in PE_PGRSs translocation in *Mtb*, or in other mycobacteria expressing ESX-5, will help to address this relevant issue.

This is of the outermost importance also in light of the conflicting results obtained in different *in vitro* and *in vivo* models implicating PE_PGRS proteins, and the ESX-5 T7SS and PPE38/PPE71 proteins, in *Mtb* virulence. Inactivation of PE_PGRS30 (Iantomasi *et al.*, 2011), ESX-5 (Bottai *et al.*, 2012; Sayes *et al.*, 2016) and MMAR_0242 (Singh *et al.*, 2016) resulted in an attenuation of *Mtb* virulence. Conversely, inactivation of PE_PGRS33 (Camassa *et al.*, 2017) and PPE38/PPE71 (Ates *et al.*, 2018), which abolished PE_PGRSs secretion, resulted in enhanced *Mtb* virulence in mice. Moreover, ESX-5 inactivation in *M. marinum* resulted in an hypervirulent phenotype in adult zebrafish (Weerdenburg *et al.*, 2012). The hypervirulent

phenotypes were associated with enhanced tissue damage and inflammation during the chronic/persistent steps of the infectious process, where the interaction between the innate and adaptive arms of the host immune system plays a key role in the dynamic equilibrium of *Mtb* infection, which can lead to overt disease or to latent infection (Barry, III *et al.*, 2009; Gengenbacher and Kaufmann, 2012; Orme, 2014). Interestingly, it has been recently proposed that PE_PGRS proteins may have evolved in *Mtb* to attenuate virulence and permit prolonged survival of the bacilli in the infected host (Ates *et al.*, 2018). The characterization of the above mentioned *Mtb* mutants in animal models or *ex vivo* human models of *Mtb* infection will be useful to improve our understanding on the role of PE_PGRS proteins in virulence.

Materials and methods

DNA manipulation and cloning strategy

Genomic DNA was extracted from liquid cultures by using the CTAB method, as described (van Embden *et al.*, 1993)**.** The *Rv0278c* and *Rv0279c* genes, expressing PE_PGRS3 and PE_PGRS4 respectively, were individually amplified from Mtb H37Rv genomic DNA using the primers indicated in Table S1.

Briefly, the forward primers were designed to anneal to 250 bp upstream of the start codon of *Rv0278c* and *Rv0279c* so to amplify their putative promoter sequence and contained the *Hind*III restriction sequence. Reverse primers were designed to anneal to the end of the gene sequence without stop codon and contained the *Xba*I or *Nhe*I restriction sequence. PCR products were obtained using the *Expand High Fidelity PCR System* (Roche) following standard procedures, cloned in pCR 2.1 TOPO T/A cloning (Life technologies) and then sequenced. Finally, both genes were inserted in the mycobacterial episomal vector (pMV206) in frame and upstream of green fluorescent protein (GFP) coding sequence and in the integrative vector (pMV306) in

frame and upstream with the haemagglutinin (HA) epitope coding sequence (Stover *et al.*, 1991).

Rv0278c gene (PE_PGRS3) and its functional mutant lacking the sequence coding the C-terminal domain (PE_PGRSΔCT) were directly amplified from the pCR vectors previously created using primers indicated in Table S1. Briefly, the forward primer was designed to anneal to the start codon of Rv0278c gene and it contained *NdeI* restriction sequence. Reverse primers were designed to anneal to different positions of the Rv0278c coding sequence and it included *NheI* adaptor sequence. PCR was carried out as previously described and products cloned in a pCR 2.1 TOPO T/A vector. Finally, Rv0278c and its gene chimeras were cloned in a modified pMV206 vector containing *hbhA* promoter upstream and the sequence coding HA epitope downstream the cloning site respectively. Furthermore, the modified pMV vector carried also the GFP sequence under control of mycobacterial antigen 85 promoter (Figure S3).

Bacterial strains, media and growth conditions and electroporation

Ms mc^2 155 and *Mtb* H37Rv were grown at 37°C in Middelbrook 7H9 broth medium (difco Becton-Dickinson), supplemented with 0.2% glycerol (Sigma-Aldrich), 10% ADC (Becton-Dichnison), and 0.05% Tween 80 (Sigma-Aldrich) using standard procedures (De Maio *et al.*, 2014; Delogu *et al.*, 2004b).

Colonies were selected on 7H11 agar media supplemented with 10% OADC (Microbiol) containing 50µg/ml hygromycin B (Sigma Aldrich) or 40µg/ml kanamycin for the strains transformed with the previously obtained vector (Table S2). Single individual antibiotic-resistant colonies were isolated and sub-cultured in a 7H9 media supplemented with 10% ADC (Microbiol) and 0.05% Tween 80 containing antibiotics concentration previously indicated and incubated at 37°C until mid-log phase. Finally, mycobacteria were stocked at -80°C after

adding 20% glycerol until use. Serial dilutions were then carried out to establish bacterial concentration.

Ms mc^2 155 grown to mid-exponential (log) phase were extensively washed with cold and sterile 10% glycerol. Two-hundred µl concentrated cells were mixed with 1µg of DNA and incubated for five minutes (m) at room temperature (RT) and then transferred to 0.2cm cuvettes (BioRad). Samples were electroporated using an electroporation system *Bio-RAD GenePulser X Cell*™ with following parameters: voltage 1250V, capacitance 25µF and resistance 800Ω (De Maio *et al.*, 2014; Palucci *et al.*, 2016). After the pulse, the cells were recovered in 1ml of liquid medium, incubated for 4 hours (h) and finally plated on 7H11 as described.

Different growth conditions considered were obtained modifying Sauton-7H9 medium or growth atmosphere gathering: Sauton standard medium; P_i depleted Sauton medium; acid (pH:5) complete 7H9 medium; iron depleted Sauton medium; magnesium depleted Sauton medium; low oxygen condition achieved by adding oil to the medium to mimic anaerobic conditions. Bacteria were grown in 48 wells plate at 37ºC.

Mycobacterial growth rate was assayed by using Mycobacteria Growth Indicator Tube (MGIT) liquid culture (Becton Dickinson). Briefly, bacteria were seeded at 10-3 cell/ml in each MGIT tube according to manufacturer's instruction. After signaled positivity, each MGIT was incubated until plateau phase. CFUs were performed at the end of the incubation and of the initial bacterial solution.

E. coli MACH 1 (Life technologies) was grown in Luria Bertani broth medium (Sigma Aldrich) or Lauria Bertani agar medium (Sigma Aldrich) according to manufacturer's standard protocol. To select transformant single colonies, ampicillin (Life technologies), hygromycin B (Sigma Aldrich) and kanamycin (Life technologies) were added at final concentration of 100 µg/ml, 150 µg/ml and 40µg/ml respectively.

SDS-PAGE, western blotting and immunoblotting

Recombinant *Ms* strains were cultured in 7H9 completed medium as previously described and then sub-inoculated in Sauton medium until mid-log phase when cells were harvested by centrifugation (4000rpm for 20 m, 4C°). To obtain whole cell lysates, cell pellets were washed with cold PBS, re-suspended in lysis buffer (20mM Tris, 150mM NaCl, 1:100 protease inhibitor cocktail, pH:7,5) and lysed by sonication five times per 5 minutes with 1 minutes in ice between each sonication (Cascioferro *et al.*, 2007; De Maio *et al.*, 2014). Proteins were separated on 12% polyacrylamide gel by SDS-PAGE and then were transferred to nitrocellulose membrane (Bio-Rad) by western blotting. Non-specific protein binding was blocked by incubating membrane into PBS containing 0,05% Tween 20 (Sigma Aldrich) and 5% Skim Milk (Oxoid) for 1 h at room temperature.

Membranes were probed with monoclonal anti-HA (1:1000) (Covance), monoclonal anti-GFP (1:5000) (Sigma Aldrich), polyclonal anti-GroEL (1:5000) (GeneTex) antibodies, and with pooled sera (1:200) obtained from mice immunized with the purified C-terminus domain (data not shown). IgG-Peroxidase (Sigma–Aldrich, Saint Louis, MO) was used as a secondary antibody. Immunoblot was developed using *Supersignal West Dura Extended Duration Substrate* (Thermo scientific) and finally chemiluminescence detected by *ChemiDoc™ XRS+ system* (Biorad).

Proteinase K treatment

Recombinant *Ms* strains were cultured in 7H9 completed medium before sub-inoculating in SAUTON medium until mid-log phase when cells were harvested by centrifugation (4000rpm for 20 minutes, 4°C). Recovered pellets were washed two times with cold PBS. Pellet was re-suspended with 2 ml of Buffer G2 (Qiagen) and then divided in two aliquots. Proteinase K (Qiagen) was added at one of the sample according to manufacturer's instruction. Both samples

were incubated in agitation for 30 minutes at RT and then they were centrifuged and washed 3 times with PBS (Bottai *et al.*, 2012). Finally, both treated and no-treated specimens were re-suspended in lysis buffer and lysed as previously indicated.

Quantitative reverse transcription - Real time PCR (qRT-PCR)

Recombinant *Ms* and *Mtb* H37Rv reference strain were grown in 7H9 supplemented medium as previously described and then sub-inoculated (1:100) in Sauton standard medium and without P_i. Cultures were incubated at 37°C and bacteria were collected for RNA extraction at different time points (15 days for *Ms* and 30-60 days for *Mtb* H37Rv). Cells were collected by centrifugation (4000rpm for 15 minutes), and RNA extracted (Soldini *et al.*, 2011). Eluted RNA was used to obtain cDNA using high capacity cDNA reverse transcription kit (Applied BioSystem).

Primers for real-time quantitative reverse transcription-PCR (qRT-PCR) specific for the 16S rRNA, *Rv2583c* (*relA*), *Rv0278c* genes were designed using primer express software (Applied BioSystem) (Table S1). Real-time quantitative PCRs were prepared with 2X SYBR master mix (Applied BioSystems) using a 7300 Real-time instrument (Applied BioSystems). 16s gene was used as housekeeping gene (Soldini *et al.*, 2011).

FACS analysis

Recombinant *Ms* expressing PE_PGRSs under their own promoters fused with GFP, *Ms* expressing only cytosolic GFP and *Ms* mc^2 155 were grown in standard Sauton medium and low phosphate Sauton medium (~50μM P_i). Ms^{GFP} and non-fluorescent wild type strains were used as controls to set the instrument. The fluorescence was analyzed at different time points using FACSCantoII flow cytometer (BD Bioscience). Briefly, careful cytometry analysis provided for a gating strategy composed by different and serial steps. Initial Forward scatter

(FSC-A) versus Side scatter (SSC-A) was carried out to identify bacteria, based on size and complexity, and to exclude debris. Progressively, two serial gating were carried out to get out doublets or inappropriate heterogeneities. Forward scatter height (FSC-H) versus FSC-A density plot and a Side scatter height (SSC-H) versus SSC-A plot were opportunely performed before measuring fluorescence. The fluorescence intensity (mycobacteria expressing GFP or PE_PGRS tagged with GFP) of 50,000 ungated events was measured as described in literature (Sureka *et al.*, 2008). Excitation laser line was at 488 nm (Excitation max value was 494 nm and emission max value was 520 nm). The data files were analyzed using *FACSDiva Software* (BD Bioscience).

Confocal microscopy and image analysis

Mycobacterial strains, grown as previously described, were plated on chamber slides pre-treated with poly-lysine (Sigma, Aldrich). Subsequently, chamber slides were incubated for 24 h at 37°C and fixed with 4% paraformaldehyde for 30 minutes before to be closed with a covered slide. Images were acquired using an inverted confocal microscope (DMIRE2, Leica microsystem, Germany) equipped with a 60X oil immersion objective. For GFP excitation a He/Ne laser exciting at 476nm was used. Internal photon multiplier tubes collected 8-bit unsigned images at 400Hz scan speed in an emission range comprised between 500 and 550nm. Image processing was performed with ImageJ software; image background value (defined as intensities below 7% of the maximum intensity) were set in zero as previously reported (De Maio *et al.*, 2014).

Total fluorescence (TF) per image has been calculated by using ImageJ software as reported (Parry and Hemstreet, III, 1988): TF = Integrated Density - (Area of image * Mean fluorescence of background) where Integrated Density is the product of Image Area and Mean Fluorescence Value. Mean fluorescence of background was calculated for each image measuring three

different empty areas (i.e. without bacteria). Average TF was calculated on five different images.

The bacterial cell length was measured using ImageJ software and at least 100 bacteria per three field were analyzed for each strain.

Images of the infected cells, previously permeabilized and marked with phalloidin-red (Life technologies), were collected using inverted microscope (Nikon Eclipse TS 100) with ADL 60X objective lens. Cells were imaged with a laser wavelength of excitation of 561 nm (emission GaAsp Detector 595/50 nm). For bacteria (GFP labeled) a laser wavelength of excitation of 488 nm was used (emission GaAsp Detector 525/50 nm). Images were then analyzed with ImageJ software.

Zeta potential measurements

Recombinant *Ms* overexpressing PE_PGRS3, and its functional mutant lacking C-terminal domain and wild type strains were grown in 7H9 medium until mid-log phase and then sub-inoculated in Sauton standard medium supplemented with kanamycin. Before performing Zeta potential analysis, each specimen was diluted in water (1:100). Solutions were characterized by Zetasizer Nano ZS (Malvern, Herrenberg, Germany) equipped with a 633 nm He–Ne laser. Universal zeta dip cell (ZEN1002, Malvern, Herrenberg, Germany) was used for experiments with a sample volume of 1 ml. For each sample, three measurements were averaged. Measurements have been done in triplicate. The Z-potential was calculated from the electrophoretic mobility by means of the Henry correction to Smoluchowski's equation as reported previously (Papi M. *et al.*, 2015).

Cell culture and mycobacteria infection

J774 murine macrophages and A549 human alveolar epithelial cells were grown in DMEM medium (Euroclone) enriched with 10% fetal bovine serum (FBS), 2mM glutamine (Euroclone), 100µg/ml streptomycin and penicillin (Euroclone) and were kept in humidified atmosphere containing 5% CO_2 at 37°C. Before infection, cells were collected and suspended in the same medium without antibiotic and supplemented with 2% FBS. Cells were plated at the concentration of 1.2 x 10^6 cell/ml and were infected after 24h at multiplicity of infection (MOI) 10:1 for 4h (5% CO_2 and 37°C) (Palucci *et al.*, 2016). Intracellular colony forming units (CFUs) were obtained at 6h post infection, whereas at 6h and 4d post infection when gentamicin was added. Images of the infected cells, previously permeabilized and marked with phalloidin-red (Life technologies), were collected using inverted microscope (Nikon Eclipse TS 100) with ADL 40X objective lens.

Murine infection

In vivo experiments were performed using 8 to 10 weeks C57/Black mice. Mice fed food and water *ad libitum* and they were housed in a temperature-controlled environment with 12h light/dark cycles. All animal experiments were approved by the Ethical Committee of the Università Cattolica del Sacro Cuore and performed in agreement with the legislative decree of the Italian Government 27 January 1992, n. 116 and the Health Minister memorandum 14 May 2001, n. 6. All manipulations were performed under isoflurane anesthesia, and all efforts were made to minimize suffering.

Five mice per group were intraperitoneally infected with 2 x 10^7 bacteria/ml of recombinant *Ms* (Figure S6). They were sacrificed at day 2 and day 6 post infection to assess spleen colonization by colonies forming unit (CFU) counting (Minerva *et al.*, 2017; Zumbo *et al.*, 2013). Supernatant deriving from spleen homogenization was used to perform bacterial counts and to evaluate cytokines pattern.

Cytokine evaluation

Supernatants of homogenized spleens were used to assay cytokine pattern after *Ms* infection. Briefly, an aliquot for each homogenized spleen was collected and centrifuged to remove tissue residues. Supernatant was then filtered to remove mycobacteria using Ultrafree-CL devices (Millipore) according to manufacturer's instruction (Camassa *et al.*, 2017). Cytokine profile was carried out by multiplex beads assay using *Bio-Plex ProTM Mouse Cytokine Th17 panel A 6-plex* (Biorad) on Bio-Plex MagPIX instrument (Biorad) according to manufacturer's instruction. All cytokine concentrations were expressed as pg/mL.

Statistical analysis

All experiments were replicated at least three times. *Microsoft Excel* (2010) and *Graphpad Prism* software version 6 (GraphPad software) were used to collect and to analyze the data. All data were expressed as mean plus SD and analyzed by one-way or two-way ANOVA comparison tests followed by the appropriate correction, as specified in the caption under each figure.

Acknowledgments: This work was supported by a grant from the Ministry of Health of Italy "Ricerca Finalizzata" RF-2011-02348713 awarded to GD and by funding from the Università Cattolica del Sacro Cuore (Linea D1).

References

Abdallah, A. M., Gey van Pittius, N. C., Champion, P. A., Cox, J., Luirink, J., Vandenbroucke-Grauls, C. M. *et al.* (2007) Type VII secretion--mycobacteria show the way. *Nat Rev Microbiol* **5:** 883-891.

Abdallah, A. M., Verboom, T., Weerdenburg, E. M., Gey van Pittius, N. C., Mahasha, P. W., Jimenez, C. *et al.* (2009) PPE and PE_PGRS proteins of Mycobacterium marinum are transported via the type VII secretion system ESX-5. *Mol Microbiol* **73:** 329-340.

Ates, L. S., Dippenaar, A., Ummels, R., Piersma, S. R., van der Woude, A. D., van der Kuij, K. *et al.* (2018) Mutations in ppe38 block PE_PGRS secretion and increase virulence of Mycobacterium tuberculosis. *Nat Microbiol* **3:** 181-188.

Barry, C. E., III, Boshoff, H. I., Dartois, V., Dick, T., Ehrt, S., Flynn, J. *et al.* (2009) The spectrum of latent tuberculosis: rethinking the biology and intervention strategies. *Nat Rev Microbiol* **7:** 845-855.

Betts, J. C., Lukey, P. T., Robb, L. C., McAdam, R. A., and Duncan, K. (2002) Evaluation of a nutrient starvation model of Mycobacterium tuberculosis persistence by gene and protein expression profiling. *Mol Microbiol* **43:** 717-731.

Biet, F., Angela de Melo, M. M., Grayon, M., Xavier da Silveira, E. K., Brennan, P. J., Drobecq, H. *et al.* (2007) Mycobacterium smegmatis produces an HBHA homologue which is not involved in epithelial adherence. *Microbes Infect* **9:** 175-182.

Bottai, D., Di, L. M., Majlessi, L., Frigui, W., Simeone, R., Sayes, F. *et al.* (2012) Disruption of the ESX-5 system of Mycobacterium tuberculosis causes loss of PPE protein secretion, reduction of cell wall integrity and strong attenuation. *Mol Microbiol* **83:** 1195-1209.

Bottai, D., Stinear, T. P., Supply, P., and Brosch, R. (2014) Mycobacterial Pathogenomics and Evolution. *Microbiol Spectr* **2:** MGM2-2013.

Boutte, C. C. and Crosson, S. (2013) Bacterial lifestyle shapes stringent response activation. *Trends Microbiol* **21:** 174-180.

Brennan, M. J. and Delogu, G. (2002) The PE multigene family: a 'molecular mantra' for mycobacteria. *Trends Microbiol* **10:** 246-249.

Brennan, M. J., Delogu, G., Chen, Y., Bardarov, S., Kriakov, J., Alavi, M. *et al.* (2001) Evidence that mycobacterial PE_PGRS proteins are cell surface constituents that influence interactions with other cells. *Infect Immun* **69:** 7326-7333.

Camassa, S., Palucci, I., Iantomasi, R., Cubeddu, T., Minerva, M., De, M. F. *et al.* (2017a) Impact of pe_pgrs33 Gene Polymorphisms on Mycobacterium tuberculosis Infection and Pathogenesis. *Front Cell Infect Microbiol* **7:** 137.

Cardona, P. J. (2009) A dynamic reinfection hypothesis of latent tuberculosis infection. *Infection* **37:** 80-86.

Cascioferro, A., Delogu, G., Colone, M., Sali, M., Stringaro, A., Arancia, G. *et al.* (2007) PE is a functional domain responsible for protein translocation and localization on mycobacterial cell wall. *Mol Microbiol* **66:** 1536-1547.

Cascioferro, A., Daleke, M. H., Ventura, M., Dona, V., Delogu, G., Palu, G. *et al.* (2011) Functional dissection of the PE domain responsible for translocation of PE_PGRS33 across the mycobacterial cell wall. *PLoS One* **6:** e27713.

Chatrath, S., Gupta, V. K., Dixit, A., and Garg, L. C. (2016) PE_PGRS30 of Mycobacterium tuberculosis mediates suppression of proinflammatory immune response in macrophages through its PGRS and PE domains. *Microbes Infect* **18:** 536-542.

Chen, T., Zhao, Q., Li, W., and Xie, J. (2013) Mycobacterium tuberculosis PE_PGRS17 promotes the death of host cell and cytokines secretion via Erk kinase accompanying with enhanced survival of recombinant Mycobacterium smegmatis. *J Interferon Cytokine Res* **33:** 452-458.

Cole, S. T., Brosch, R., Parkhill, J., Garnier, T., Churcher, C., Harris, D. *et al.* (1998) Deciphering the biology of Mycobacterium tuberculosis from the complete genome sequence. *Nature* **393:** 537-544.

De Maio, F., Maulucci, G., Minerva, M., Anoosheh, S., Palucci, I., Iantomasi, R. *et al.* (2014) Impact of protein domains on PE_PGRS30 polar localization in Mycobacteria. *PLoS One* **9:** e112482.

Delogu, G. and Brennan, M. J. (1999) Functional domains present in the mycobacterial hemagglutinin, HBHA. *J Bacteriol* **181:** 7464-7469.

Delogu, G., Bua, A., Pusceddu, C., Parra, M., Fadda, G., Brennan, M. J. *et al.* (2004a) Expression and purification of recombinant methylated HBHA in Mycobacterium smegmatis. *FEMS Microbiol Lett* **239:** 33-39.

Delogu, G., Pusceddu, C., Bua, A., Fadda, G., Brennan, M. J., and Zanetti, S. (2004b) Rv1818c-encoded PE_PGRS protein of Mycobacterium tuberculosis is surface exposed and influences bacterial cell structure. *Mol Microbiol* **52:** 725-733.

Delogu, G., Sanguinetti M, Pusceddu, C., Bua, A., Brennan, M. J., Zanetti, S. *et al.* PE_PGRS proteins are differentially expressed by Mycobecterium tuberculosis in host tissue. Microbes and infection 8, 2061-2067. 5-6-2006.

Delogu, G., Manganelli, R., and Brennan, M. J. (2014) Critical research concepts in tuberculosis vaccine development. *Clin Microbiol Infect* **20 Suppl 5:** 59-65.

Delogu, G., Brennan, M. J., and Manganelli, R. (2017) PE and PPE Genes: A Tale of Conservation and Diversity. *Adv Exp Med Biol* **1019:** 191-207.

Deng, W., Long, Q., Zeng, J., Li, P., Yang, W., Chen, X. *et al.* (2017) Mycobacterium tuberculosis PE_PGRS41 Enhances the Intracellular Survival of M. smegmatis within Macrophages Via Blocking Innate Immunity and Inhibition of Host Defense. *Sci Rep* **7:** 46716.

Dheenadhayalan, V., Delogu, G., and Brennan, M. J. (2006a) Expression of the PE_PGRS 33 protein in Mycobacterium smegmatis triggers necrosis in macrophages and enhanced mycobacterial survival. *Microbes Infect* **8:** 262-272.

Dheenadhayalan, V., Delogu, G., Sanguinetti, M., Fadda, G., and Brennan, M. J. (2006b) Variable expression patterns of Mycobacterium tuberculosis PE_PGRS genes: evidence that PE_PGRS16 and PE_PGRS26 are inversely regulated in vivo. *J Bacteriol* **188:** 3721-3725.

Dickson, J. S. and Koohmaraie, M. (1989) Cell surface charge characteristics and their relationship to bacterial attachment to meat surfaces. *Appl Environ Microbiol* **55:** 832-836.

Elks, P. M., Brizee, S., van, d., V, Walmsley, S. R., van Eeden, F. J., Renshaw, S. A. *et al.* (2013) Hypoxia inducible factor signaling modulates susceptibility to mycobacterial infection via a nitric oxide dependent mechanism. *PLoS Pathog* **9:** e1003789.

Elliott, S. R. and Tischler, A. D. (2016a) Phosphate responsive regulation provides insights for ESX-5 function in Mycobacterium tuberculosis. *Curr Genet* **62:** 759-763.

Elliott, S. R. and Tischler, A. D. (2016b) Phosphate starvation: a novel signal that triggers ESX-5 secretion in Mycobacterium tuberculosis. *Mol Microbiol* **100:** 510-526.

Espitia, C., Laclette, J. P., Mondragon-Palomino, M., Amador, A., Campuzano, J., Martens, A. *et al.* (1999) The PE-PGRS glycine-rich proteins of Mycobacterium tuberculosis: a new family of fibronectin-binding proteins? *Microbiology* **145 (Pt 12):** 3487-3495.

Fattorini, L., Piccaro, G., Mustazzolu, A., and Giannoni, F. (2013) Targeting dormant bacilli to fight tuberculosis. *Mediterr J Hematol Infect Dis* **5:** e2013072.

Gengenbacher, M., Rao, S. P., Pethe, K., and Dick, T. (2010) Nutrient-starved, non-replicating Mycobacterium tuberculosis requires respiration, ATP synthase and isocitrate lyase for maintenance of ATP homeostasis and viability. *Microbiology* **156:** 81-87.

Gengenbacher, M. and Kaufmann, S. H. (2012) Mycobacterium tuberculosis: success through dormancy. *FEMS Microbiol Rev* **36:** 514-532.

Gey van Pittius, N. C., Sampson, S. L., Lee, H., Kim, Y., van Helden, P. D., and Warren, R. M. (2006) Evolution and expansion of the Mycobacterium tuberculosis PE and PPE multigene families and their association with the duplication of the ESAT-6 (esx) gene cluster regions. *BMC Evol Biol* **6:** 95.

Houben, E. N., Bestebroer, J., Ummels, R., Wilson, L., Piersma, S. R., Jimenez, C. R. *et al.* (2012) Composition of the type VII secretion system membrane complex. *Mol Microbiol* **86:** 472-484.

Hyyrylainen, H. L., Pietiainen, M., Lunden, T., Ekman, A., Gardemeister, M., Murtomaki-Repo, S. *et al.* (2007) The density of negative charge in the cell wall influences two-component signal transduction in Bacillus subtilis. *Microbiology* **153:** 2126-2136.

Iantomasi, R., Sali, M., Cascioferro, A., Palucci, I., Zumbo, A., Soldini, S. *et al.* (2011) PE_PGRS30 is required for the full virulence of Mycobacterium tuberculosis. *Cell Microbiol*.

Lamarche, M. G., Wanner, B. L., Crepin, S., and Harel, J. (2008) The phosphate regulon and bacterial virulence: a regulatory network connecting phosphate homeostasis and pathogenesis. *FEMS Microbiol Rev* **32:** 461-473.

Lim, A., Eleuterio, M., Hutter, B., Murugasu-Oei, B., and Dick, T. (1999) Oxygen depletion-induced dormancy in Mycobacterium bovis BCG. *J Bacteriol* **181:** 2252-2256.

Manganelli, R. (2014) Sigma Factors: Key Molecules in Mycobacterium tuberculosis Physiology and Virulence. *Microbiol Spectr* **2:** MGM2-2013.

Menozzi, F. D., Bischoff, R., Fort, E., Brennan, M. J., and Locht, C. (1998) Molecular characterization of the mycobacterial heparin-binding hemagglutinin, a mycobacterial adhesin. *Proc Natl Acad Sci U S A* **95:** 12625-12630.

Minerva, M., De, M. F., Camassa, S., Battah, B., Ivana, P., Manganelli, R. *et al.* (2017) Evaluation of PE_PGRS33 as a potential surface target for humoral responses against Mycobacterium tuberculosis. *Pathog Dis* **75**.

Monu and Meena, L. S. (2016) Biochemical characterization of PE_PGRS61 family protein of Mycobacterium tuberculosis H37Rv reveals the binding ability to fibronectin. *Iran J Basic Med Sci* **19:** 1105-1113.

Orme, I. M. (2014) A new unifying theory of the pathogenesis of tuberculosis. *Tuberculosis (Edinb)* **94:** 8-14.

Pai, M., Behr, M. A., Dowdy, D., Dheda, K., Divangahi, M., Boehme, C. C. *et al.* (2016) Tuberculosis. *Nat Rev Dis Primers* **2:** 16076.

Palucci, I., Camassa, S., Cascioferro, A., Sali, M., Anoosheh, S., Zumbo, A. *et al.* (2016) PE_PGRS33 Contributes to Mycobacterium tuberculosis Entry in Macrophages through Interaction with TLR2. *PLoS One* **11:** e0150800.

Papi M, Lauriola M.C., Palmieri V., Ciasca G., Maulucci G., and De Spirito M. (2015) Plasma protein corona reduces the haemolytic activity of graphene oxide nano and micro flakes. RSC Advances 5, 81638-81641.

Parry, W. L. and Hemstreet, G. P., III (1988) Cancer detection by quantitative fluorescence image analysis. *J Urol* **139:** 270-274.

Peddireddy, V., Doddam, S. N., and Ahmed, N. (2017) Mycobacterial Dormancy Systems and Host Responses in Tuberculosis. *Front Immunol* **8:** 84.

Pethe, K., Alonso, S., Biet, F., Delogu, G., Brennan, M. J., Locht, C. *et al.* (2001) The heparin-binding haemagglutinin of M. tuberculosis is required for extrapulmonary dissemination. *Nature* **412:** 190-194.

Phelan, J. E., Coll, F., Bergval, I., Anthony, R. M., Warren, R., Sampson, S. L. *et al.* (2016) Recombination in pe/ppe genes contributes to genetic variation in Mycobacterium tuberculosis lineages. *BMC Genomics* **17:** 151.

Primm, T. P., Andersen, S. J., Mizrahi, V., Avarbock, D., Rubin, H., and Barry, C. E., III (2000) The stringent response of Mycobacterium tuberculosis is required for long-term survival. *J Bacteriol* **182:** 4889-4898.

Rengarajan, J., Bloom, B. R., and Rubin, E. J. (2005) Genome-wide requirements for Mycobacterium tuberculosis adaptation and survival in macrophages. *Proc Natl Acad Sci U S A* **102:** 8327-8332.

Rifat, D., Bishai, W. R., and Karakousis, P. C. (2009) Phosphate depletion: a novel trigger for Mycobacterium tuberculosis persistence. *J Infect Dis* **200:** 1126-1135.

Russell, D. G., Cardona, P. J., Kim, M. J., Allain, S., and Altare, F. (2009) Foamy macrophages and the progression of the human tuberculosis granuloma. *Nat Immunol* **10:** 943-948.

Saini, N. K., Baena, A., Ng, T. W., Venkataswamy, M. M., Kennedy, S. C., Kunnath-Velayudhan, S. *et al.* (2016) Suppression of autophagy and antigen presentation by Mycobacterium tuberculosis PE_PGRS47. *Nat Microbiol* **1:** 16133.

Sayes, F., Pawlik, A., Frigui, W., Groschel, M. I., Crommelynck, S., Fayolle, C. *et al.* (2016) CD4+ T Cells Recognizing PE/PPE Antigens Directly or via Cross Reactivity Are Protective against Pulmonary Mycobacterium tuberculosis Infection. *PLoS Pathog* **12:** e1005770.

Serafini, A., Boldrin, F., Palu, G., and Manganelli, R. (2009) Characterization of a Mycobacterium tuberculosis ESX-3 conditional mutant: essentiality and rescue by iron and zinc. *J Bacteriol* **191:** 6340-6344.

Serafini, A., Pisu, D., Palu, G., Rodriguez, G. M., and Manganelli, R. (2013) The ESX-3 secretion system is necessary for iron and zinc homeostasis in Mycobacterium tuberculosis. *PLoS One* **8:** e78351.

Silhavy, T. J., Kahne, D., and Walker, S. (2010) The bacterial cell envelope. *Cold Spring Harb Perspect Biol* **2:** a000414.

Singh, P. P., Parra, M., Cadieux, N., and Brennan, M. J. (2008) A comparative study of host response to three Mycobacterium tuberculosis PE_PGRS proteins. *Microbiology* **154:** 3469-3479.

Singh, V. K., Berry, L., Bernut, A., Singh, S., Carrere-Kremer, S., Viljoen, A. *et al.* (2016) A unique PE_PGRS protein inhibiting host cell cytosolic defenses and sustaining full virulence of Mycobacterium marinum in multiple hosts. *Cell Microbiol* **18:** 1489-1507.

Soldini, S., Palucci, I., Zumbo, A., Sali, M., Ria, F., Manganelli, R. *et al.* (2011) PPE_MPTR genes are differentially expressed by Mycobacterium tuberculosis in vivo. *Tuberculosis (Edinb)* **91:** 563-568.

Song, H. and Niederweis, M. (2012) Uptake of sulfate but not phosphate by Mycobacterium tuberculosis is slower than that for Mycobacterium smegmatis. *J Bacteriol* **194:** 956-964.

Stover, C. K., de la Cruz, V. F., Fuerst, T. R., Burlein, J. E., Benson, L. A., Bennett, L. T. *et al.* (1991) New use of BCG for recombinant vaccines. *Nature* **351:** 456-460.

Sureka, K., Ghosh, B., Dasgupta, A., Basu, J., Kundu, M., and Bose, I. (2008) Positive feedback and noise activate the stringent response regulator rel in mycobacteria. *PLoS One* **3:** e1771.

Tischler, A. D., Leistikow, R. L., Kirksey, M. A., Voskuil, M. I., and McKinney, J. D. (2013) Mycobacterium tuberculosis requires phosphate-responsive gene regulation to resist host immunity. *Infect Immun* **81:** 317-328.

Tufariello, J. M., Chapman, J. R., Kerantzas, C. A., Wong, K. W., Vilcheze, C., Jones, C. M. *et al.* (2016) Separable roles for Mycobacterium tuberculosis ESX-3 effectors in iron acquisition and virulence. *Proc Natl Acad Sci U S A* **113:** E348-E357.

van de Weerd, R., Boot, M., Maaskant, J., Sparrius, M., Verboom, T., van Leeuwen, L. M. *et al.* (2016) Inorganic Phosphate Limitation Modulates Capsular Polysaccharide Composition in Mycobacteria. *J Biol Chem* **291:** 11787-11799.

van Embden, J. D., Cave, M. D., Crawford, J. T., Dale, J. W., Eisenach, K. D., Gicquel, B. *et al.* (1993) Strain identification of Mycobacterium tuberculosis by DNA fingerprinting: recommendations for a standardized methodology. *J Clin Microbiol* **31:** 406-409.

Walters, S. B., Dubnau, E., Kolesnikova, I., Laval, F., Daffe, M., and Smith, I. (2006) The Mycobacterium tuberculosis PhoPR two-component system regulates genes essential for virulence and complex lipid biosynthesis. *Mol Microbiol* **60:** 312-330.

Wayne, L. G. (1954) Growth of Mycobacterium tuberculosis from resected specimens under various atmospheric conditions. *Am Rev Tuberc* **70:** 910-911.

Wayne, L. G. (2001) In Vitro Model of Hypoxically Induced Nonreplicating Persistence of Mycobacterium tuberculosis. *Methods Mol Med* **54:** 247-269.

Weerdenburg, E. M., Abdallah, A. M., Mitra, S., de, P. K., van der Wel, N. N., Bird, S. *et al.* (2012) ESX-5-deficient Mycobacterium marinum is hypervirulent in adult zebrafish. *Cell Microbiol* **14:** 728-739.

Weiss, G. and Schaible, U. E. (2015) Macrophage defense mechanisms against intracellular bacteria. *Immunol Rev* **264:** 182-203.

World Health Organization. Global tuberculosis report 2017. 2017.

Yang, W., Deng, W., Zeng, J., Ren, S., Ali, M. K., Gu, Y. *et al.* (2016a) Mycobacterium tuberculosis PE_PGRS18 enhances the intracellular survival of M. smegmatis via altering host macrophage cytokine profiling and attenuating the cell apoptosis. *Apoptosis*.

Ying Huang, Y. W. Y. B. Z. G. W. L. Y. D. Z. Expression of PE_PGRS 62 protein in Mycobacterium smegmatis decrease mRNA expression of proinflammatory cytokines IL-1b, IL-6 in macrophages. Mol Cell Biochem 340, 223-229. 10-2-2010.

Zumbo, A., Palucci, I., Cascioferro, A., Sali, M., Ventura, M., D'Alfonso, P. *et al.* (2013) Functional dissection of protein domains involved in the immunomodulatory properties of PE_PGRS33 of Mycobacterium tuberculosis. *Pathog Dis* **69:** 232-239.

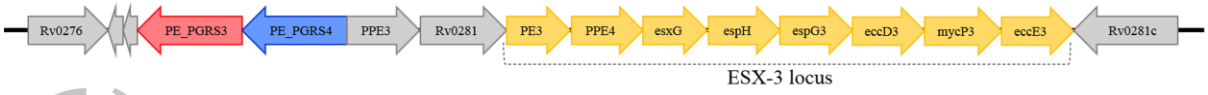

Figure 1. Schematic representation of the *Rv0278c* and *Rv0279* gene locus of *Mtb* H37Rv.

PE_PGRS3 (red) and PE_PGRS4 (blue) are localized near the ESX-3 system (yellow arrows).

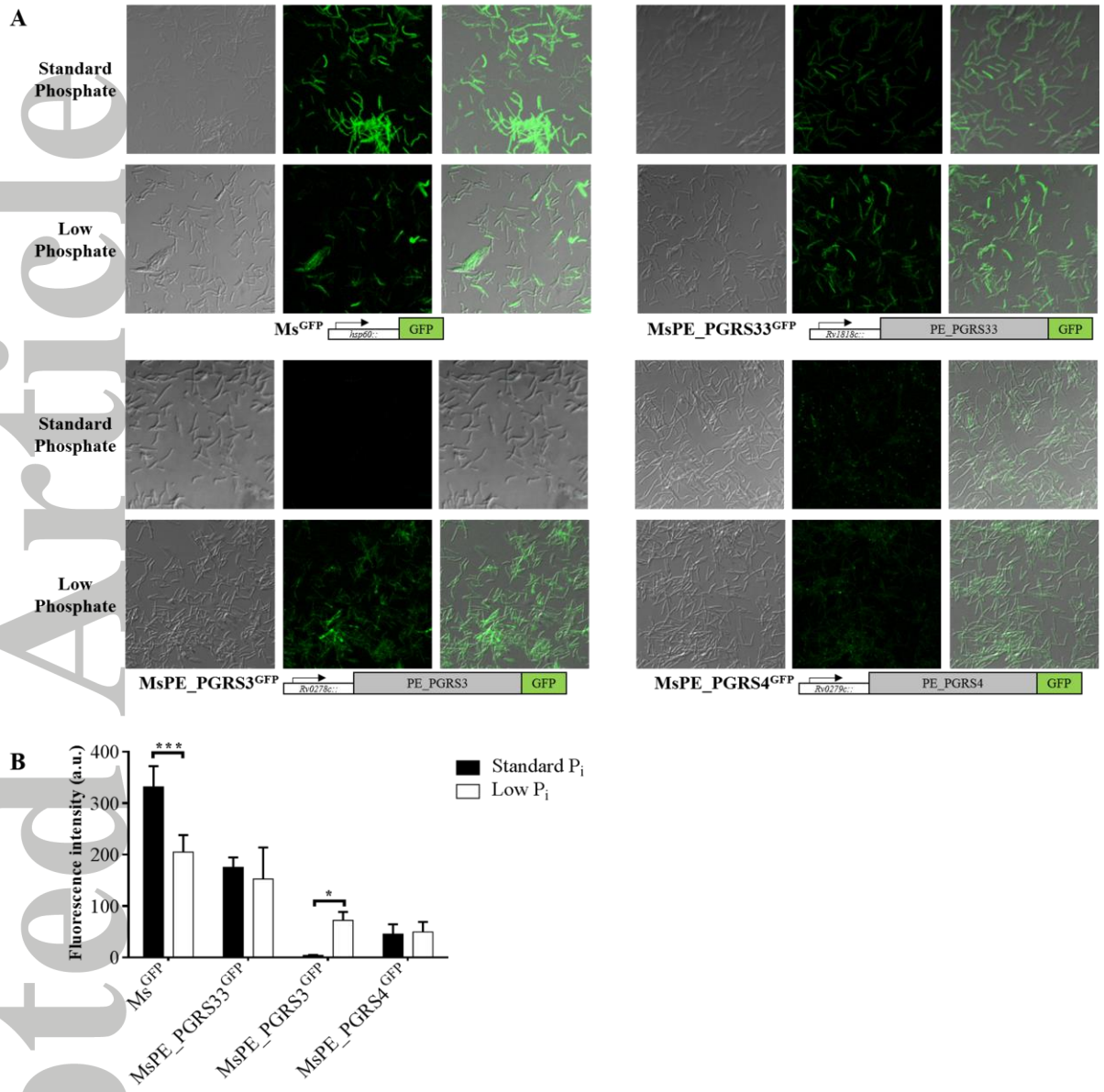

Figure 2. Confocal microscopy images and fluorescence intensity analysis. *Mycobacterium smegmatis* (*Ms*) expressing PE_PGRS3, PE_PGRS4, PE_PGRS33, all tagged with the green fluorescent protein (GFP) at C-terminus (*Ms*PE_PGRS3^{GFP}, *Ms*PE_PGRS4^{GFP} and *Ms*PE_PGRS33^{GFP}), and *Ms* expressing cytosolic GFP (*Ms*^{GFP}) were grown in standard and low inorganic phosphate (P_i) media. Following 15 days of incubation transmittance (on the left) and green channel (centre) images were acquired. Overlapping (on the right) was carried out with ImageJ software (**A**)**.** Fluorescence intensity analysis of the images was performed by

using ImageJ software (**B**), after having removed background noise. Statistical analysis was carried out by two-way ANOVA with Tukey's correction.

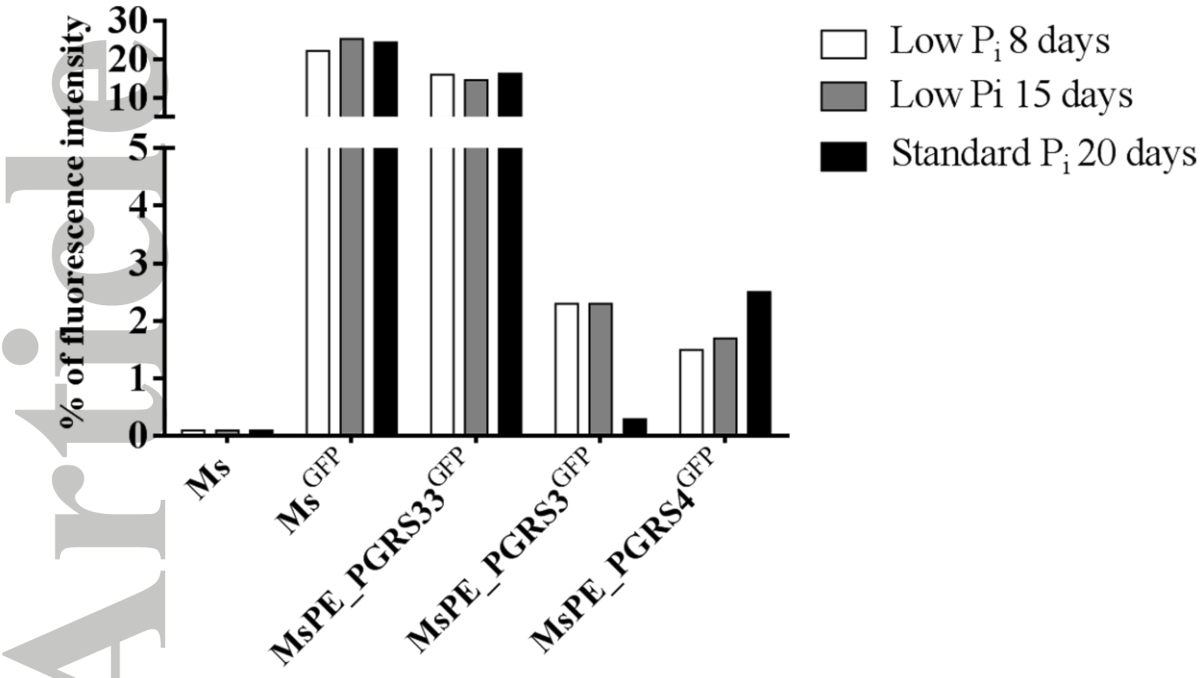

Figure 3. Kinetic of PE_PGRS3 and PE_PGRS4 expression in low P_i media. Inorganic phosphate (P_i) dependent expression of PE_PGRS3, PE_PGRS4, PE_PGRS33 (*Ms*PE_PGRS3^{GFP}, *Ms*PE_PGRS4^{GFP} and *Ms*PE_PGRS33^{GFP}) was assessed by FACS analysis. *Ms* mc155 and *Ms*^{GFP} (expressing cytosolic green fluorescent protein, GFP) were used as negative and positive controls, respectively. All strains were grown in low P_i Sauton medium and measurements were acquired at different time points. On day 15, bacterial cells were washed and re-suspended in fresh Sauton medium containing standard concentration of P_i and fluorescence measured until day 20.

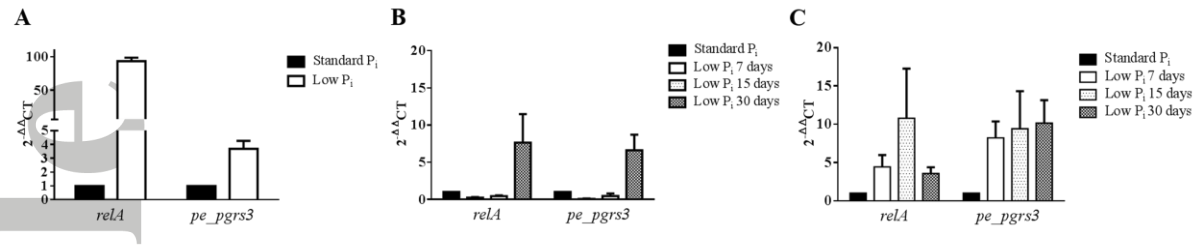

Figure 4. Real time PCR analysis. **(A)** PE_PGRS3 and its relationship with starving environment was evaluated assaying *pe_pgrs3* and *relA* expression. Real time PCR was carried out on *Ms*PE_PGRS3^{GFP} expressing PE_PGRS3 under its putative promoter tagged with the green fluorescent protein (GFP). Bacteria were grown in Sauton medium with standard inorganic phosphate (P_i) and low P_i (~50µM) for 15 days. *relA* and *pe_pgrs3* gene expression was assayed in standard medium and in phosphate starvation. Target cDNA was internally normalized to 16s cDNA. Expression of *pe_pgrs3* and *relA* genes in *Mtb* H37Rv **(B)** and *MtbΔSigE* **(C)** was assayed in standard P_i and low P_i (~50µM) at 7, 15 and 30 days. Target cDNA was again normalized to 16s cDNA.

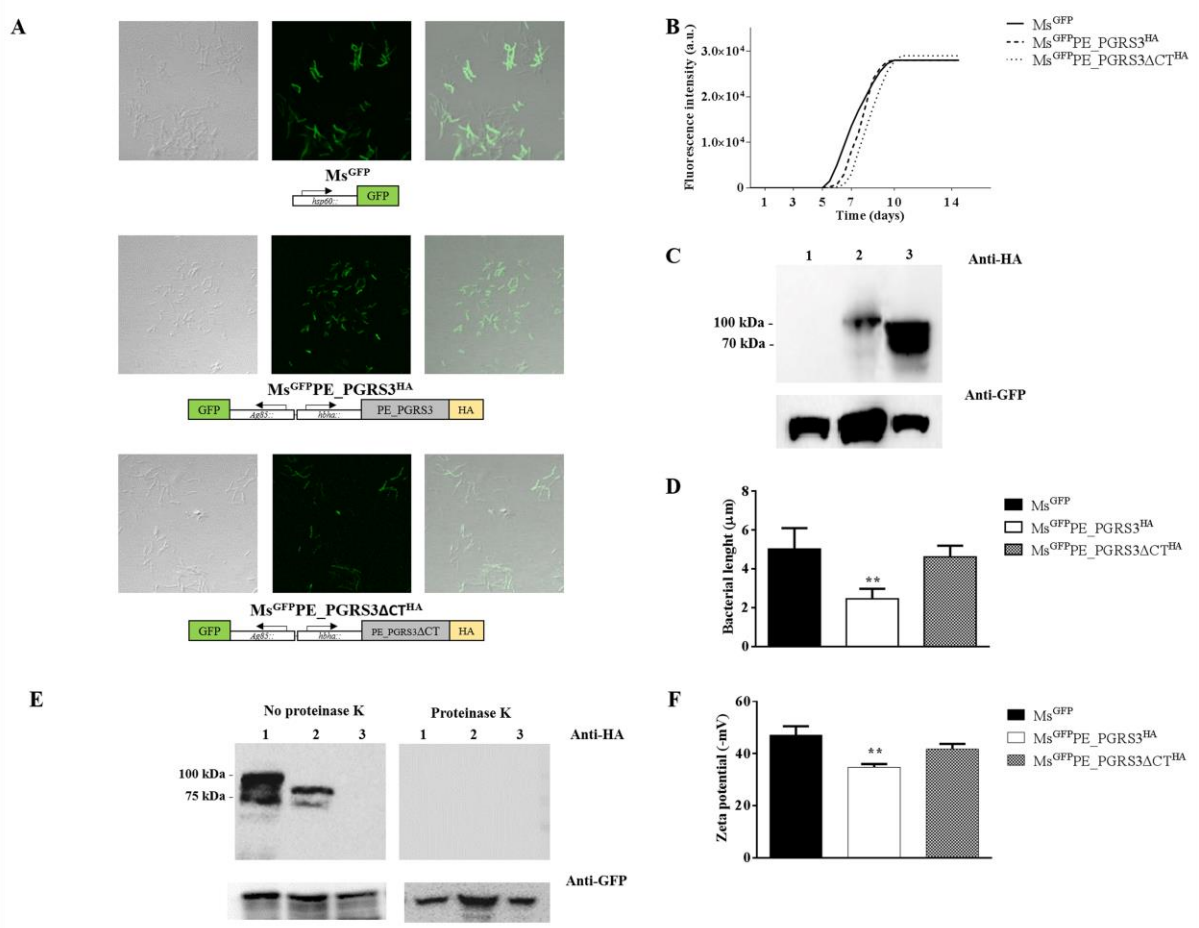

Figure 5. Analysis of recombinant *Ms* over-expressing PE_PGRS3 chimeras. (**A**) Confocal microscopy images of *Ms* expressing cytosolic GFP (*Ms*^{GFP}), full length PE_PGRS3 and its chimera lacking of C-terminus domain (*Ms*^{GFP}PE_PGRS3^{HA} and *Ms*^{GFP}PE_PGRS3ΔCT^{HA} respectively). Both PE_PGRS3 and its functional domain were tagged with HA epitope. Green channel was acquired using Nikon confocal microscope with 60X objective (1 pixel = 0,21µm) and analyzed with ImageJ software. (**B**) Bacterial growth rate of *Ms*^{GFP}, *Ms*^{GFP}PE_PGRS3^{HA} and *Ms*^{GFP}PE_PGRS3ΔCT^{HA} performed in Mycobacteria Growth Indicator Tube (MGIT). Measured fluorescence intensity (a.u.) and days of culture were reported to obtain the growth profile. (**C**) Immunoblot was carried out with anti-HA monoclonal antibodies and with anti-GFP polyclonal antibodies and represents whole cell lysate of *Ms*^{GFP}, *Ms*^{GFP}PE_PGRS3 (81Kda), *Ms*^{GFP}PE_PGRS3ΔCT (71Kda) in lane 1, 2, 3 respectively. (**D**) Bacterial cell length

analysis, using ImageJ software, showed that *Ms*^{GFP}PE_PGRS3^{HA} is smaller in size (50%) than *Ms*^{GFP} and *Ms*^{GFP}PE_PGRS3ΔCT^{HA} ($p<0.0001$). (**E**) Immunoblot of the whole cell lysates of above mentioned recombinant *Ms* strains after treating cells with proteinase K or not. Immunoblot was probed by using anti-HA monoclonal antibody. Monoclonal anti-GFP polyclonal antibodies were used as lysis control. Lane 1, 2 and 3 represent whole cell lysates of *Ms*^{GFP}PE_PGRS3^{HA}, *Ms*^{GFP}PE_PGRS3ΔCT^{HA} and *Ms*^{GFP} respectively. C-terminus domain appears surfaced exposed. (**F**) Mycobacterial surface charge, indicated with Z-potential of *Ms*^{GFP} and *Ms*^{GFP}PE_PGRS3^{HA} and *Ms*^{GFP}PE_PGRS3ΔCT^{HA}, was performed by Light scattering assay. Bacterial strains were cultured in Sauton medium and then diluted 1:100 before the experiment. Media of measures of the surface charge of three different experiments were analyzed. *Ms*^{GFP}PE_PGRS3^{HA} showed a less negative surface charge than other strains ($p<0.01$).

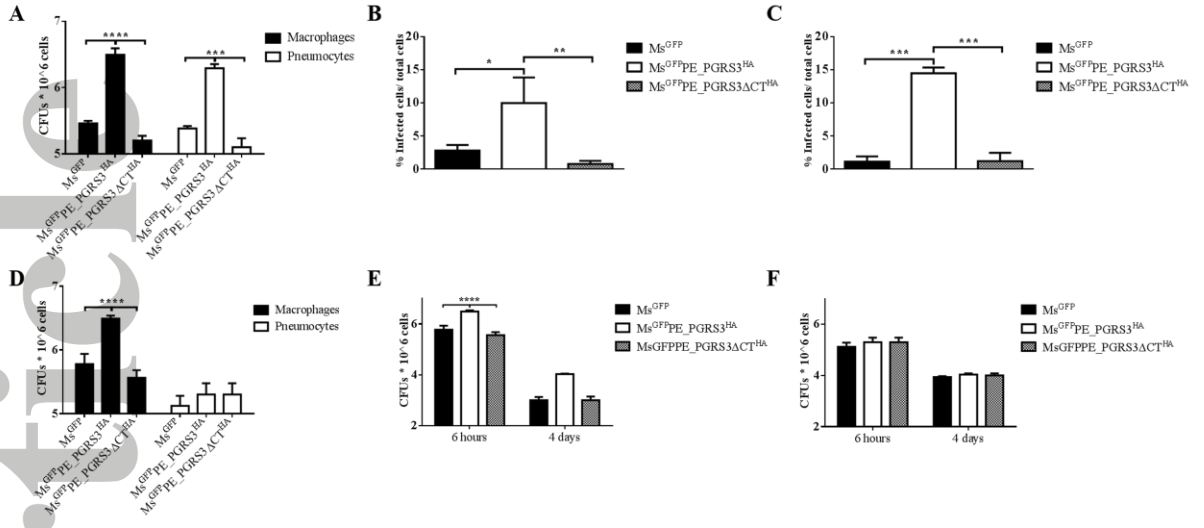

Figure 6. CFUs after infection of murine macrophages (J774) and human alveolar epithelial cells (A549). Bacterial entry phenotype was evaluated by infecting murine macrophages (J774) and human alveolar epithelial cells (A549) with *Ms* recombinant strains at (MOI 10:1) without adding antibiotic (**A**, **B**, **C**) or with gentamicin (**D**, **E**, **F**). J774 and A549 were infected as previously described with *Ms*^{GFP}, *Ms*^{GFP}PE_PGRS3^{HA} and *Ms*^{GFP}PE_PGRS3ΔCT^{HA} strains, after four hours cells were washed and new media was added. CFUs were evaluated after two hours and a significant result was obtained for *Ms*^{GFP}PE_PGRS3^{HA} in both cellular types ($p<0.0001$) **(A)**. Murine macrophages **(B)** and human alveolar epithelial **(C)** infected cells on total cells amount were analyzed using confocal microscopy. *Ms*^{GFP}PE_PGRS3^{HA} showed a greater percentage of infected cells in both cell lines. Conversely, the infected cells were washed at 4 hours post infection, new sterile medium containing gentamicin was added, and the plates were incubated for 2 hours to remove extracellular growth of the adhered bacteria. Finally, CFUs were evaluated 2h after adding the antibiotic and a significant result was obtained for *Ms*^{GFP}PE_PGRS3^{HA} in macrophages ($p<0.0001$) but not in epithelial cells showed that the full-length PE_PGRS3 mediates entry in macrophages but not in epithelial cells **(D)**. Survival of *Ms*^{GFP}, *Ms*^{GFP}PE_PGRS3^{HA} and *Ms*^{GFP}PE_PGRS3ΔCT^{HA} in J774 **(E)** and A549 **(F)** was evaluated 4 days post infection. No

significant differences were observed between the two time points. Data are representative of a single experiment repeated three times. CFUs are reported in $\log_{10}$ scale.

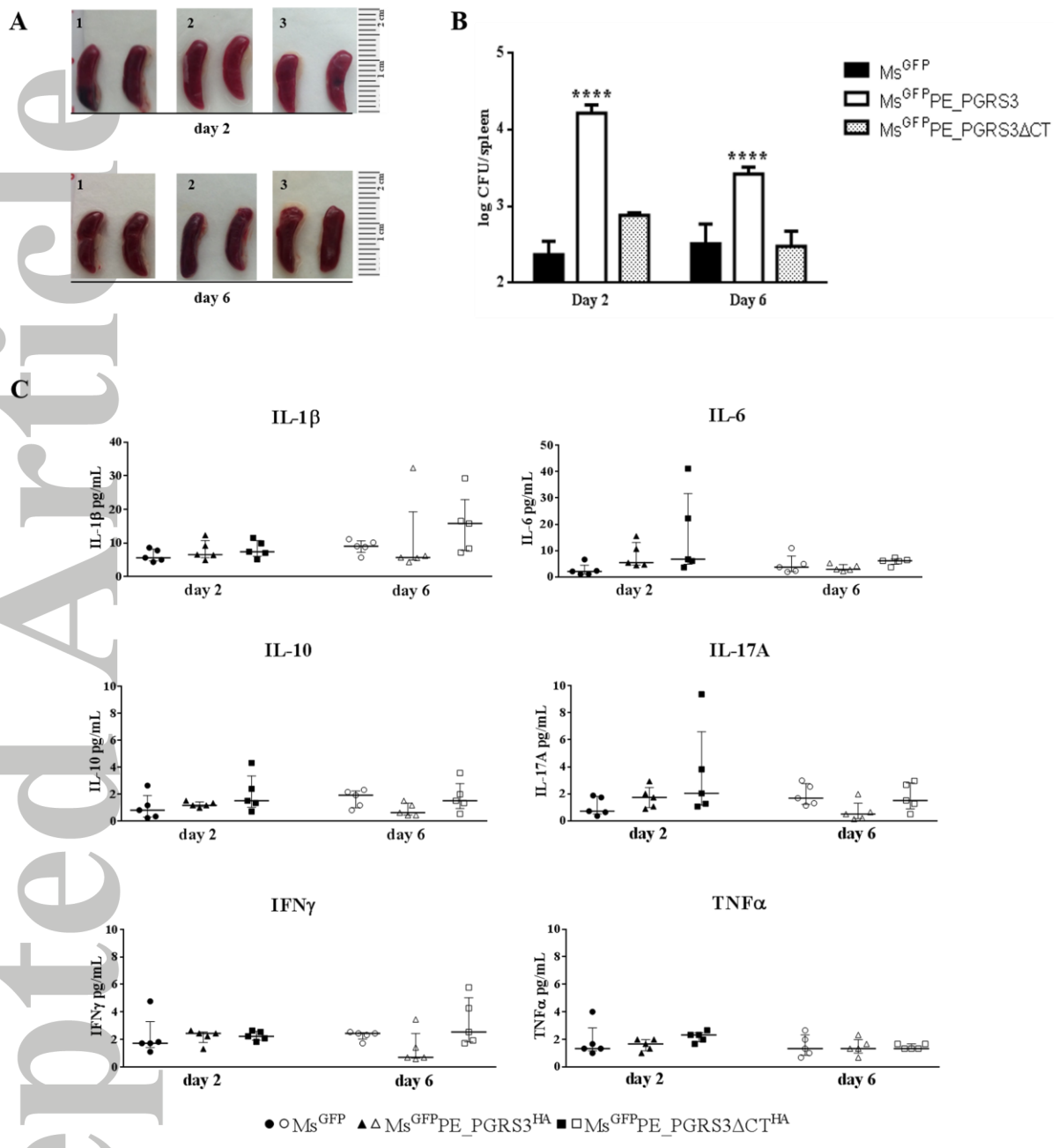

Figure 7. Spleen colonization after infection with the recombinant *Ms* strains expressing PE_PGRS3 chimeras and cytokine evaluation. C57Bl/6 mice were intra-peritoneally infected ($2x10^7$ bacteria/ml) with *Ms* strains expressing PE_PGRS3 chimeras (*Ms*^{GFP}PE_PGRS3^{HA}, *Ms*^{GFP}PE_PGRS3ΔCT^{HA} and *Ms*^{GFP}). Mice were sacrificed at day 2 and day 6 post infection and spleens were aseptically removed and then homogenized in 5 ml of sterile phosphate buffer (PBS). No differences in size or aspect were observed between the three groups of mice (representative images) **(A)**. Higher CFUs were observed in the spleen of

mice infected with *Ms*^{GFP}PE_PGRS3^{HA} compared to Ms parental strain or the *Ms*^{GFP}PE_PGRS3ΔCT^{HA} ($p<0.0001$) at both time points **(B)**. Cytokines were evaluated by filtering supernatants of homogenized spleens by multiplex beads assay. No significant differences were observed in the three groups of mice **(C)**. Data are representative of a single experiment repeated three times. CFUs are reported in $\log_{10}$ scale.